Glow Discharge Optical Emission Spectroscopy – The Fundamental Principles

Kazuaki Wagatsuma

The Institute for Materials Research, Tohoku University, Katahira 2-1-1, Sendai 980-8577, Japan

(Received August 8, 1997)

ABSTRACT

Some of the fundamental principles of glow discharges: the structure of the discharges, cathode sputtering, and light emission, are described, including the excitation and ionization phenomena occurring in the glow discharge plasma. The glow discharge tube with a flat cathode (Grimm-style), which is commonly available for the emission spectrometric analysis, is introduced together with a table of the sensitive emission lines of various elements.

1. INTRODUCTION

In 1967, Walter Grimm introduced a glow discharge tube with a flat cathode for spectrochemical analysis /1,2/. The analytical potentialities of this device have been investigated by many authors and some fundamental properties have also been studied. Some review articles on these subjects have been published /3-5/. In the Grimm-style glow discharge tube, the possibility of in-depth profiles using a planar sample has attracted many researchers who are interested in surface elemental analysis. The release of analyte atoms from the cathode surface is governed by cathode sputtering. The sputtering phenomenon, which was first observed by Plucker at the cathode of a glow discharge /6/, has since been the subject of many studies /7/. The noticeable characteristics of cathode sputtering are less dependent on the properties of the sample used; the sputtering yield principally determines the production of particles ejected from the sample surface. Furthermore,

the excitation and ionization processes occurring in the glow discharge have also been studied /8,9/, contributing to the understanding of optical emission from this device.

In this paper, two major features of the glow discharge excitation source: cathode sputtering and excitation and ionization mechanisms in low-pressure glow discharges, are described in view of their importance in the analytical application.

2. GLOW DISCHARGES

Though a gaseous body usually exists as a very stable insulator, breakdown phenomena are sometimes observed in concentrated electric power, such as in thunder and lightning or in a short-circuit spark. Low pressure glow discharges pertinent to the interests here are also a typical breakdown phenomenon in a conducting ionized gas. Direct current glow discharges are produced at reduced pressures of several hundred Pa and discharge voltages of some hundreds of volts, and can be self-sustained under certain self-stabilized discharge conditions.

A low pressure glow discharge can be produced using a sealed glass vessel provided with two electrodes set parallel, as illustrated by Francis /10/ in Fig. 1. The chamber has a port for connecting it with a vacuum system and an inlet port for introducing a discharge gas. The chamber is evacuated and then filled with the discharge gas, which is usually an inert gas such as argon, and a dc potential V is applied across the two electrodes. It is essential in understanding the behavior

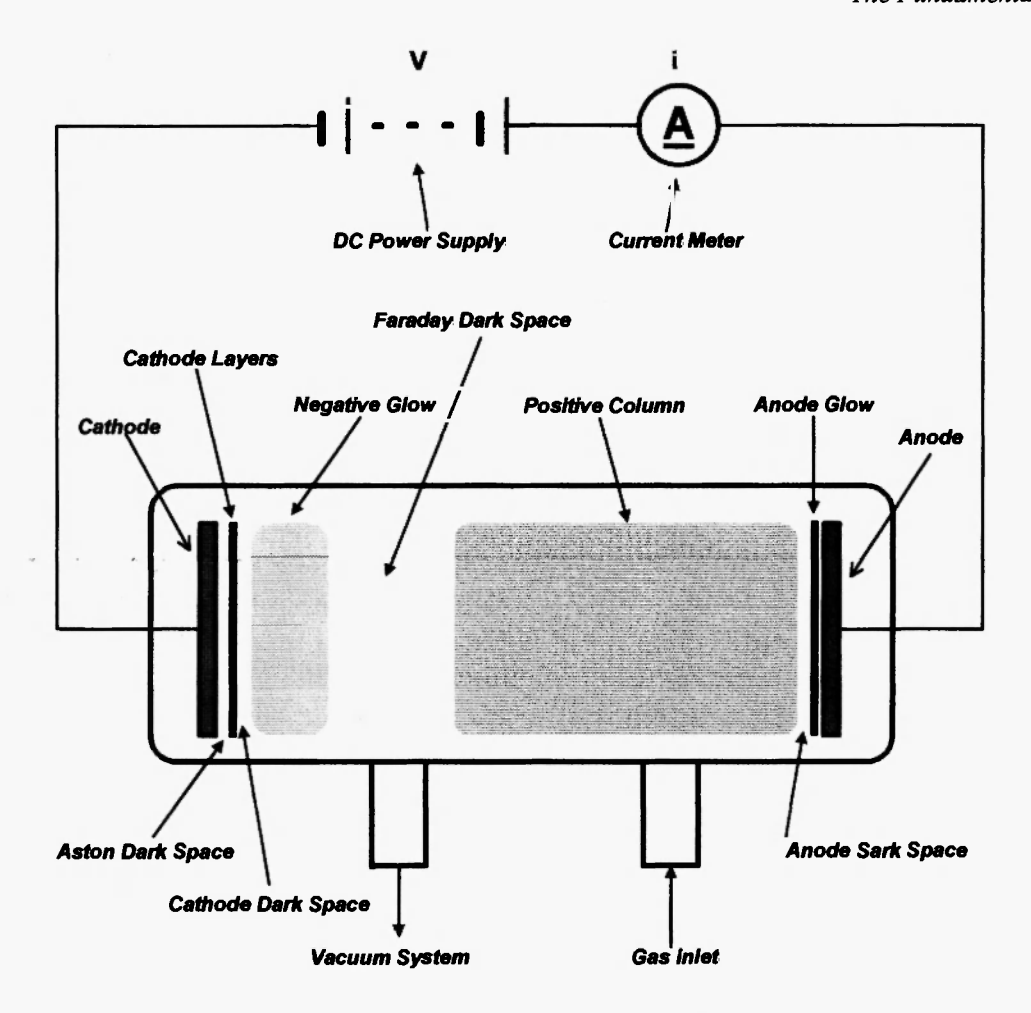


Fig. 1: Schematic structure of a dc glow discharge.

of the discharge to investigate the variation in the discharge current i as a function of the applied voltage V; such a variation is called the voltage-current characteristic of the discharge.

Figure 2 illustrates a typical example of the V-I characteristics of the glow discharge, shown by Penning /11/. Initially no current flow is observed if the applied voltage is too low to induce ionization in the gaseous body. As the dc potential V is gradually raised, an unstable and intermittent discharge accompanied by random sparks may be observed at very low values of the current (also called dark current). If the potential V is further increased, the discharge current i increases rapidly and a dark self-maintained discharge is produced. Such a discharge is known as a Townsend dark discharge (the region A-B), which is characterized by a so-called breakdown voltage V_b. The breakdown

voltage for the self-sustained discharge relates to the density of charged particles such as electrons in the gaseous body. Initial electrons and gas ions, which exist even when no electric field is applied, are accelerated and subsequently collide with gas particles. A part of these particles is ionized through various collisions, such as electron impact, and then the resultant charged particles can also contribute to further ionization collisions. If the density of the charged particles is low, ion recombination and diffusion to the container walls dominate and thus the current dissipated is not accompanied by any visible radiation. The density of the charged particles increases as the result of a chain of such ionization collisions, and finally the breakdown phenomenon occurs when the degree of ionization exceeds a certain threshold value.

When the discharge current further increases, the

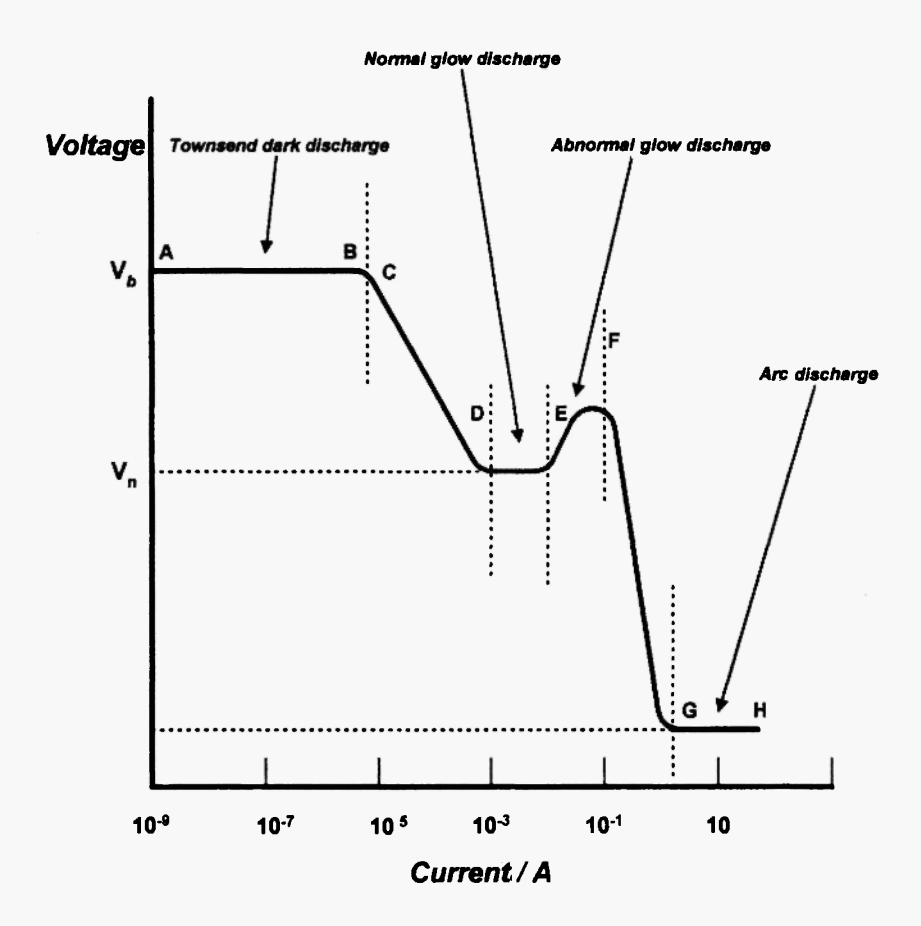


Fig. 2: Typical voltage-current characteristics of a dc glow discharge /11/.

voltage decreases (the region C-D) and reaches a constant value Vn. The potential Vn then remains almost constant for large variations of the current from about 10⁻⁴ A to 10⁻² A (the region D-E). In such discharges, one can observe zones in the discharge body from which visible light is strongly emitted. When the discharge current is more than the value at the point E in Fig. 2, the voltage again varies and the discharge enters the region where the discharge voltages increase along with the current (the region E-F). The discharges in the region D-E-F in Fig. 2 are called glow discharges. The former is called a "normal" glow and the latter an "abnormal" glow /12/. If the current is raised above the value at point F, the discharge voltage decreases abruptly and then reaches only several tens of volts for currents of the order of 10 A. This indicates that the discharge characteristics are altered from high voltage/ low current (glow discharge) to low voltage/high current (region G-E) called arc discharge. In analytical applications, it is the glow discharge in the abnormal

region rather than the normal region that is employed as the light excitation source.

It is well known that the glow discharge in the chamber comprises several alternating dark and luminous zones, as indicated in Fig. 1/10/. However, all of these zones do not always appear in the glow discharge column. The structure may be varied by the geometry of the chamber, especially the distance between the two electrodes. In general, when the electrode distance is relatively long, the positive column (the luminous zone near the anode) attracts much attention in the discharge column. However, the positive column is not essential for maintaining the glow discharge. It is found that, if the space between the electrodes is reduced, the positive column shrinks and finally disappears while the negative glow (the luminous zone near the cathode) and the cathode dark space are hardly affected. In this case, the Faraday dark space as well as the positive column also disappears. Such a discharge is called an "obstructed" glow /12/.

It should be noted that discharge tubes working under the obstructed glow conditions are employed extensively as an excitation source for atomic emission spectrometry /3-5,13-15/. Chapman suggested a simplified but fundamental structure model, which includes only the negative glow, the cathode dark space, and the anode dark space, as illustrated in Fig. 3 /8/. In this model, a glow region occupies the greater part of the discharge body and the dark spaces are adjacent to each electrode. The anode dark space is much thinner than the cathode dark space. The lower graph of Fig. 3 indicates schematically the voltage distribution when the anode electrode is grounded. Little electric potential is evident in the glow region, and thus most of this

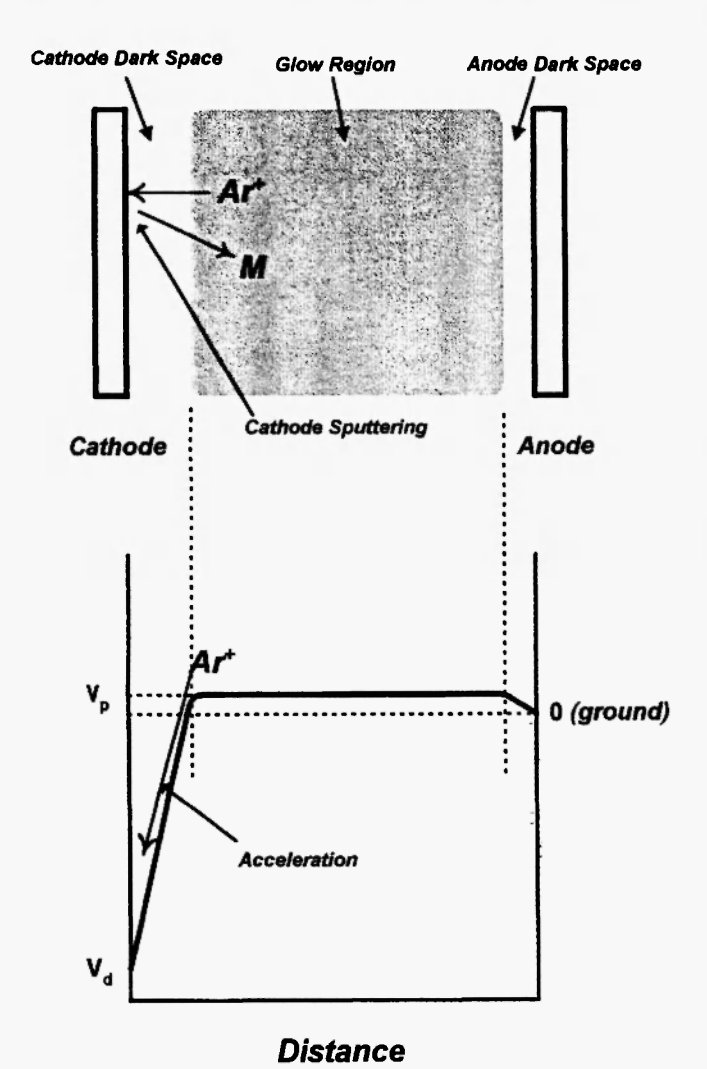


Fig. 3: Voltage distribution in an obstructed dc glow discharge /8/, and schematic explanation of cathode sputtering.

region has the same potential V_p , called the plasma potential. The glow region is at a small positive potential (typically 10 V) with respect to the grounded anode. The reason for this is that there is a great difference in the mobility between an electron and an ion in the glow discharge /8/.

Since a negative potential corresponding to the voltage V_d is applied to the cathode, an electric field is produced in the cathode dark space. The difference in the potential across the cathode dark space is called the cathode fall. In the anode dark space, the plasma potential V_p can induce an electric field though its strength is much smaller than that of the cathode dark space. The electric fields in the discharge body are largely restricted to the dark spaces at each of the electrodes. Electrons not having sufficient kinetic energies to penetrate these fields are repelled back towards the negative glow region not only by the cathode dark space field.

Electrons in the discharge body are accelerated by the applied electric field and subsequently the energetic electrons collide with gas atoms to cause the ionization. While a great number of electrons are produced as a result of various collisional reactions, the electrons are lost rapidly through electron-ion recombination processes. It is likely that the discharge is sustained by counterbalancing between the creation and the loss rate of the electrons. Further, there is also a considerable energy loss by heat from the discharge body to the environment. To obtain a steady state discharge, the energy loss must be compensated for by the energetic electrons because only these electrons are capable of accepting electric energies from the external power supply.

As shown in Fig. 3, the cathode surface is exposed to bombardment of the positive ions which are accelerated by the electric field in the cathode dark space, which causes the ejection of cathode atoms (sputtering). At the same time, released energies from the bombarding ions also enable electrons to be ejected from the cathode surface. Such electrons are called γ -electrons /16/ or secondary electrons. In glow discharges, the γ -electrons become a primary source of electrons needed to maintain the discharge. Electrons which emanate from the electrodes by heating play a

major role in the maintenance of arc or spark discharges, whereas the heat-induced electrons are relatively few in the glow discharges.

The efficiency of the γ -electron emission varies with the kind and the kinetic energy of the bombarding ion, the kind of cathode material, the surface state of the cathode, and so on. The efficiency γ_i is defined as the number of electrons ejected per incident ion. In general, the γ_i s of insulator cathodes are greater than those of metals, and the γ_i s of clean metallic cathodes are not so different /8,12/. However, the effect of surface contamination such as oxidation or gas adsorption seems to be remarkably great, leading to a variation in the V-I characteristics of glow discharges due to the type of surface layer on the cathode.

The strong electric field corresponding to the cathode fall repels the y-electrons from the cathode through the negative glow zone towards the anode, and the repelled electrons may acquire energies enough to ionize the gas particles. Though the ionization by the energetic electrons occurs in the cathode dark space, the number of resultant charged particles is not enough to maintain the discharge. It is considered that the main source of ionization may not be the cathode dark space but the negative glow region Considerable amounts of electrons and ions are produced in the negative glow region principally through electron impact ionization The intense emission from the glow, including radiations from the sputtered particles from the cathode in addition to those from the discharge gas, results from excitation collisions with the numerous secondary electrons having appropriate kinetic energies. These emissions from the sputtered materials are analyzed in glow discharge optical emission spectrometry /3-5, 13-15/.

Some of the created gas ions are attracted towards the cathode surface by the electric field in the cathode dark space and act as primary ions in cathode sputtering. In the glow region, metastable gas atoms — atoms in an excited state having a long lifetime — are also produced, and these contribute to the ionization and excitation processes.

Electrons in the glow region can be classified into at least three different groups /8/. The first group consists of the γ -electrons which enter from the cathode dark

space with relatively high energies, named primary electrons. The second group consists of the electrons which are created secondarily in the negative glow, named secondary electrons. The last group consists of the electrons which are repelled by the anode dark space field as well as by the cathode dark space field. Eventually, the slow electrons are trapped by the plasma potential because of their low kinetic energies. However, because these occupy larger parts of the glow electrons, the average kinetic energy of the glow electrons, or specifically, the electron temperature, is determined mainly by the last group of electrons. It was reported that the electron temperature ranges from a few eV to 0.1 eV /8,17/.

The primary electrons have much higher kinetic energies than the secondary electrons, but their density is rather lower /10/. Many of the energies which the primary electrons have cannot be transmitted to the discharge body because the cross-section regarding an electron collision is fairly low /12/. Most of the primary electrons run away to the anode surface without any loss of their kinetic energies, and eventually their energies result in heating there. However, a small share only of their energies is essential for maintenance of the glow discharge.

The secondary electrons resulting from ionizing collisions have considerably lower energies, but some of them have appropriate kinetic energies for excitation of particles in the glow discharges. Intense radiations from the negative glow are excited principally by collisions with the numerous secondary electrons, or by collisions with metastable gas atoms which have previously been excited.

3. GLOW DISCHARGE PLASMA

The plasma state produced by glow discharges is a so-called weakly-ionized gaseous body /12/. A typical degree of ionization is 1% of the neutral articles in the plasma. Accordingly, the density of the charged particles such as electrons is fairly low compared to that of the neutral particles. In most cases, the glow discharges are able to be maintained under an evacuated atmosphere at the pressure of several Torr, which implies that the probability of collisions among the

Property	Neutral atom	Ion	Electron
Density	high	low	low
Kinetic energy (temperature)	low	low	high
Internal energy	can conserved (metastable)	conserved (ionization potential)	cannot conserved

Table 1
Properties of particles in the glow discharge plasma

particles is small.

Table 1 summarizes the properties of the three major particles in the glow discharges, i.e., neutral atom, ion, and electron The difference in the population between the neutral and the charged particles is due to the small probability of ionization It should be noted that the average kinetic energy differs greatly between the electron and the neutral atom. In other words, the electron temperature (T_e) is considerably higher than the gas temperature (T_e). In low-pressure discharge plasmas including the glow discharge plasma, the T_e is not very elevated even in comparison with ambient temperatures /17/, whereas the T_e may be more than 10000 K.

Only charged particles can receive external energy from the electric field of the glow discharges, and neutral particles, which virtually form most of the plasma body, are provided energy only indirectly through various collisions. It is deduced from the theory of elastic collision /12/ that the transfer of collisional energy from electrons to the atomic particles is performed much less effectively than in the collisions between massy particles like neutral atoms. It is therefore required that electron-particle collisions must occur more frequently in the plasma, in order that the kinetic energy of the electron may be transferred completely. However, in the glow discharge plasma, this requirement is not realized because of the low density of

particles in the plasma. As a result, electrons are predominantly accelerated but a large part of the acquired energy cannot be transferred to the massy particles such as neutral atoms because of insufficient energy exchanges. In other words, the glow discharge plasma is not in local thermodynamic equilibrium (LTE) /18/. Under non-LTE conditions, it is difficult to define a characteristic temperature which can explain various processes and reactions occurring in the plasma.

4. EXCITATION AND DE-EXCITATION PROCESSES IN THE GLOW DISCHARGE PLASMA

The excitation and de-excitation phenomena of atoms are caused by energy exchanges in the various collisions occurring in the plasma. The collisional reactions are classified broadly into those of the first kind and those of the second kind /19/. The kinetic energies of particles are exchanged in collisions of the first kind, whereas, in the second kind, internal energies are used which certain kinds of the particles can store. There is no collision of the second kind in which an electron provides the excitation energy, because an electron has no internal energy. On the other hand, particles having internal energy exist as neutral atoms

(molecules) as well as ions. Large parts of the excited particles having higher energy are de-excited rapidly down to the lower energy states with the emission of a photon, and then the lifetime of these states is much shorter than the time required for energy exchanges by means of any inter-particle collision or of collisions to the walls /20/. However, in a particular excited state called a metastable state, any de-excitation process followed by the photon emission is forbidden by selection rules /20/. The particle in the metastable state has a prolonged lifetime, and may survive until it is de-excited through the radiationless processes. It can therefore be considered that a metastable state has an internal energy corresponding to its excitation energy. Especially in low pressure discharges, the density of metastables is expected to be raised due to the relatively low probability of the inter-particle collisions.

Table 2 indicates that rare gases, which are usually used as the plasma gas in the glow discharge spectroscopy, have important metastable energy levels. For example, a neutral argon atom has two metastable levels, i.e., $4s[3/2]_2$ (11.55 eV) and $4s[1/2]_0$ (11.83 eV) /21/, and singly-ionized argon in the ground state has the internal energy corresponding to the first ionization potential, i.e., $3p^2P_{3/2}$ (15.76 eV) and $3p^2_{1/2}$ (15.94 eV)

/21/. These metastable states can act as energy donors in the collisional energy transfer occurring in the glow discharge plasma.

Typical collisional reactions can be represented by the following equations /11/:

$$A + D(fast) \rightarrow A^{+} + D(slow) + \Delta E$$
 (1)

$$A + D(fast) \rightarrow (A^{\dagger})^{\dagger} + D(slow) + e^{-} + \Delta E$$
 (1')

$$A + e^{-}(fast) \rightarrow A^{+} + e^{-}(slow) + \Delta E$$
 (2)

$$A + e^{-}(fast) \rightarrow (A^{+})^{2} + e^{-}(slow) + e^{-} + \Delta E$$
 (2')

$$A + D^{m} \rightarrow (A^{+})^{2} + D^{g} + e^{-} + \Delta E$$
 (3)

$$A + D^{+} \rightarrow (A^{+})^{\bullet} + D^{g} + \Delta E \tag{4}$$

where the superscript denoted by g, m, *, or $\bar{}$, represents ground, metastable, excited, and ionic state, respectively. On receiving the energy from a particle **D** (or an electron e), a particle **A** is excited and immediately de-excited with the photon emission. ΔE denotes the difference in the excitation energy before and after the collision.

Table 2
Metastable levels of rare gases /21/

Element	Metastable Level	Ionization Energy
Helium	1s2s ³ S ₁ (19.82 eV)	1s ² S _{i.2} (24.58 eV)
	1s2s ¹ S ₀ (20.61 eV)	
Neon	2s3s [3/2], (16.62 eV)	$2p^2P_{3/2}(21.56 \text{ eV})$
	2s3s [1/2] ₀ (16.85 eV)	$2p^{2}P_{1/2}(21.66 \text{ eV})$
Argon	3s4s [3/2] ₂ (11.55 eV)	$3p^2P_{3/2}(15.76 \text{ eV})$
	3s4s [1/2] ₀ (11.83 eV)	$3p^{2}P_{1/2}(15.94 \text{ eV})$

Equations (1) and (2) show the collisions of the first kind where the excitation and ionization reactions are caused by *fast* particles having sufficient kinetic energy. It is required that the kinetic energy is greater than the excitation (or ionization) energy of the energy acceptor A. Equations (3) and (4) show the collisions of the second kind where the excitation and ionization reactions are caused by the metastables having sufficient internal energies.

As described in the previous section, the gas temperature of the glow discharge plasma is not high, so that kinetic reactions such as equation (1) take place less actively. This implies that atom-atom or atom-ion collisions are minor processes for obtaining excited species in the plasma. On the other hand, the electron impact collision denoted by equation (2) can be a possible mechanism for the excitation and ionization in the glow discharge plasma. Primary electrons which are accelerated from the cathode sheath to the negative glow region have lower density, although they have higher kinetic energy. Ultimate electrons which are trapped in the negative glow occupy larger parts of the overall electrons in the plasma /8/. The average kinetic energy of the ultimate electron is within a few eV /8/, and it can be consumed for excitation of the colliding partner.

Equation (3) is called Penning ionization /12/. In this case, the metastable particle $\mathbf{D}^{\mathbf{m}}$ acts as an energy donor for the ionization of the particle \mathbf{A} , and the surplus energy $\Delta \mathbf{E}$ is taken away mainly by the ejected electron. Penning ionization by rare gases is a feasible process in the glow discharge plasmas because the metastable levels are populated under the evacuated atmosphere.

Equation (4) is known as a charge transfer ionization /22/. It should be noted that no electron is released in this reaction. The surplus energy ΔE is added to the kinetic energy of the colliding particles but it is rather difficult for such an energy transfer to occur compared to the conversion to the kinetic energy of an electron. As a result, the charge transfer process is most likely to take place when ΔE is very small, indicating that an energy resonance is needed /9,22/.

Emission spectra from LTE plasmas may be explained with a characteristic temperature. However, it is difficult in a non-LTE plasma to understand the emission spectrum only with an idea of the plasma

temperature. It has been reported that spectrum patterns emitted from the glow discharge plasma are strongly dependent on the kind of plasma gas employed /23-26/. The characteristics of the gas determine not only the relative intensities of the emission lines but the kinds of observable spectral lines. Metastable species of the plasma gas play significant roles in exciting emission lines of singly-ionized atoms /23/.

As an example, we now consider the emission spectrum of copper. Figure 4 shows spectral scans of copper obtained with a Grimm-style glow discharge source when three different gases, i.e., argon, neon, and nitrogen, are employed as the plasma gas /24/. The spectrum patterns differ from each other to the extent that one might judge them not to be from a common sample (copper). The difference is attributed to the emission lines of singly-ionized copper (ionic lines). The spectrum (Fig. 4(c)) from the nitrogen plasma comprises some emission lines of neutral copper (atomic lines) and emission bands of N₂ species, but the ionic lines hardly appear. The spectrum from the argon (Fig. 4(a)) as well as the neon plasma (Fig. 4(b)) includes the ionic lines in addition to the atomic lines. It is further found that major ionic lines obtained with argon gas are different from those with neon

The ionic lines from the argon plasma are assigned to the transition from the 3d⁹4p (8.23-8.66 eV) to the 3d⁹4s (2.12-2.98 eV) excited state, whereas, in the neon plasma, the transition from the 3d⁹5s (13.39-13.68 eV) to the 3d⁹4p state results in intense ionic lines /25/. It should be noted that in the argon plasma the Cull 224.77 nm line whose upper state is the 4p ³P₂ level (8.235 eV) is extremely strong. The 4p ³P₂ level has the lowest excitation energy of the excited levels originating from the 3d⁹4p state. A schematic energy diagram of singly-ionized copper in Fig. 5 shows that the 4p ³P₂ level can be populated greatly through the charge transfer reaction between singly-ionized argon and the ground state of copper atom due to good matching in the excitation energies, which enables the Cull 224.77 nm line to be very intense /27/. Similarly, in the neon plasma, the population of the 3d⁹5s excited levels can be raised through the charge transfer reaction between singly-ionized neon and the ground state of copper atom /28,29/. It is possible to detect, in the glow discharge plasma containing helium gas, the emission

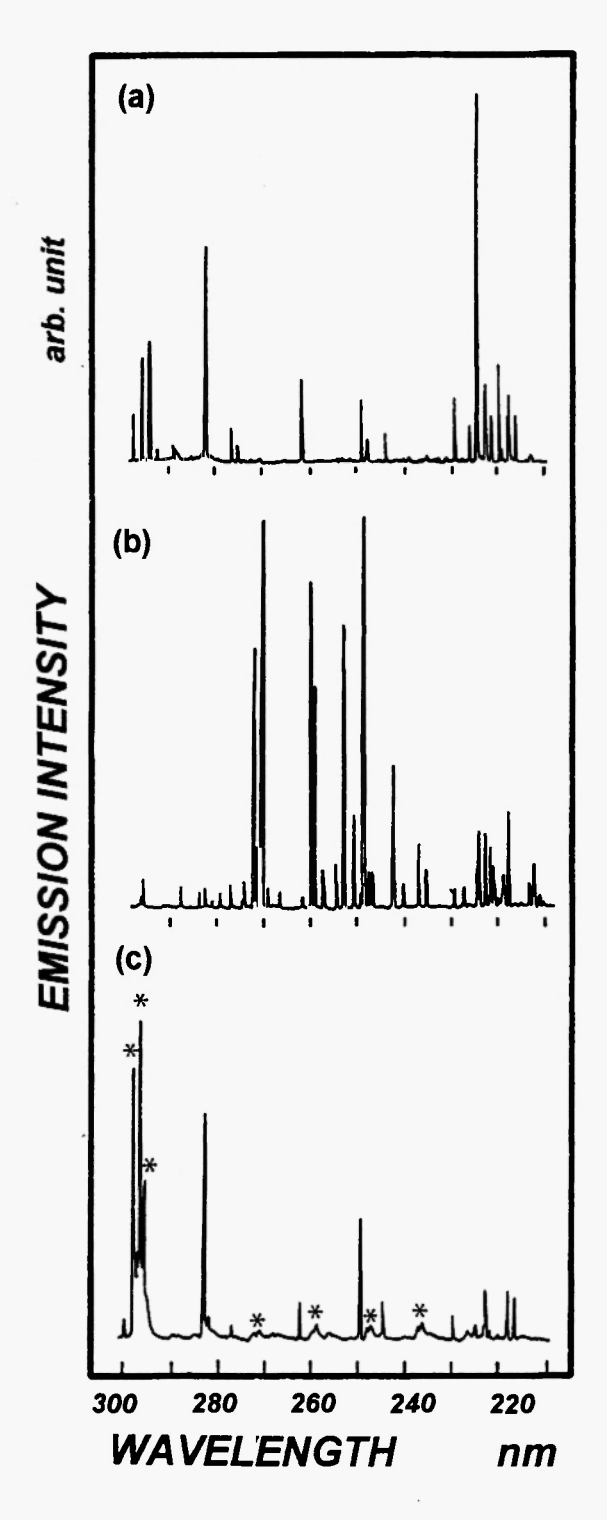


Fig. 4: Spectral scans of copper in the wavelength range from 210 to 300 nm recorded with (a) Ar, 400 V.19.5 mA, (b) Ne, 550 V/11.2 mA, and (c) N₂ 550 V/15.4 mA /24/. The lines due to N₂ gas are marked with asterisks.

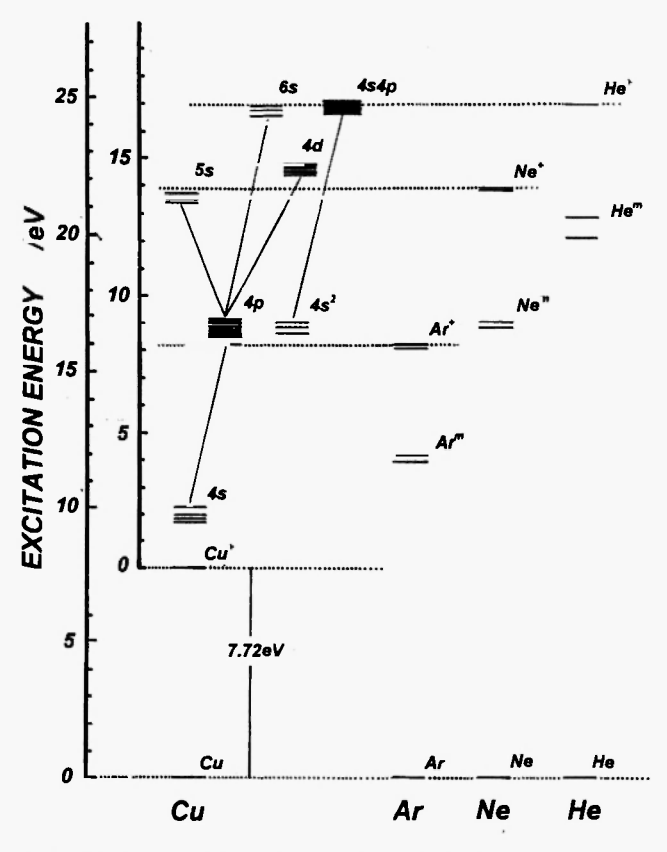


Fig. 5: Schematic energy level diagram of singlyionized copper, together with the metastable levels of rare gases /25/.

lines whose upper energy levels are the 6s and the 4s4p states having higher excitation energies /30/.

The selective excitation to particular excited levels is a typical non-LTE process occurring in the glow discharge plasma. Hence extremely intense emission lines are observed. The charge transfer collision is a significant mechanism for the excitation when there is energy resonance between internal energies of the colliding partners.

4. CATHODE SPUTTERING

As illustrated in Fig. 3, positive ions and fast neutrals strike the cathode surface, penetrating a few atomic distances while losing their kinetic energy through a sort of three-dimensional billiards cascade of atomic lattice collisions. Some atoms at the uppermost surface receive sufficient energy through these collisions to overcome their binding energy and are normally ejected as neutral atoms, although a small percentage may be ejected as ions. Positive ions are returned to the surface by the strong electric field in the cathode sheath; however, a certain amount of the neutral atoms can diffuse into the negative glow region. Glow discharge analytical method is based on optical emission of the sputtered neutral atoms in the glow region.

Sputtering yield, which is defined as the number of atoms ejected from a target surface per incident ion /7/, is the most fundamental parameter of the sputtering processes. It depends on the mass, the energy, and the incident angle of the bombarding ion, the mass of the target atom, and the chemical and physical states of the surface. It is known that there is a threshold for sputtering (20 eV to 40 eV) that is approximately equal to the heat of sublimation /31,32/. Above the threshold for sputtering, the yields increase with incident energy of the bombarding ions and reach a broad maximum in the energy region of 5 to 50 keV /32/. The decrease in the sputtering yields at higher energies is related to the larger penetration of the ion into the target, and the

sputtering cannot be explained by the cascade collisions /33/. Table 3 shows the sputtering yields of various elements at the incident energy of 600 eV, reported by Wehner et al. /34,35/. Higher mass particles give generally larger sputtering yields than lower mass ones. However, the sputtering yields are typically 0.1 to 5 indicating that the difference in sputtering yield among the elements is not very large.

The sputtering yield determines the erosion rate of the cathode sample. In glow discharges, the bombarding ions are by no means monoenergetic, and it is not necessarily valid to use yield data for pure elements when alloys, compounds, or mixtures are sputtered. It has been reported that the sputtering yields in alloy samples are often different from those predicted from the pure samples /32/. Despite these effects, the published data concerning sputtering yields are still available, if one roughly estimates erosion rate that might be expected for a given material /36,37/.

In the glow discharges, flow of the bombarding ions cannot be focused; however, wide and uniform sampling can be done over the whole of the sample sputtered (typically 0.1 cm²). The bottom shape of the sputtered surface is almost flat, except for the edge of the crater /38/. Furthermore, the sputtering rate is

Table 3
Sputtering yields of elements at the incident energy of 600 eV /34,35/

Target		In	cident ion		
	Не	Ne	Ar	Kr	Xe
C	0.085			0.18	0.21
Al	0.021	0.83	1.24	1.11	1.02
Si	0.15	0.54	0.53	0.64	0.51
Ti	0.08	0.45	0.58	0.53	0.50
V	0.09	0.55	0.70	0.69	0.72
Cr	0.20	1.05	1.30	1.55	1.90
Fe	0.17	0.97	1.26	1.23	1.20
Co	0.15	0.99	1.36	1.33	1.30
Ni	0.18	1.34	1.52	1.55	1.48
Cu	0.27	2.00	2.30	2.80	2.44
Ag	0.23	1.98	3.40	3.90	4.20

relatively high (typically 1 μ m /min) because of the large density of the bombarding ions, which means that the glow discharge device is especially suited for the analysis of thick layers, such as electrodeposited or hot-dipped metal coatings /39-41/.

5. GRIMM-STYLE GLOW DISCHARGE TUBE

The Grimm-style glow discharge tube /1,2/ is most often employed as an excitation source in analytical emission spectroscopy. Figure 6 illustrates a schematic diagram of the discharge tube /42/. The sample is taken as the cathode, and the hollow anode is kept a small distance from the cathode sample (typically 0.2-0.3 mm). The discharge tube is first evacuated down to 10⁻² Torr by two rotary vacuum pumps; subsequently, a discharge gas, usually argon, is introduced in the tube at a pressure of several Torr and flows continuously during the measurement. When a voltage is applied between the two electrodes (typically several hundred volt), a glow discharge is produced in front of the cathode. The radiation is measured by end-on observation.

The Grimm-style glow discharge is classified into the obstructed glow discharge. A steady discharge can develop in the narrow region between the inner wall of the anode and the part of the cathode located opposite the hollow anode cavity, as shown in Fig. 6. The bright part of the discharge consists mainly of the negative glow. In analytical applications, the zone of interest is the negative glow because the particles sputtered from the cathode sample are strongly excited in this zone to emit the spectra of the neutral and ionized atoms. The positive column and the anode glow, which are not needed to maintain the glow discharge, have been eliminated by reducing the distance between the two electrodes.

The current-voltage characteristic of this discharge was reported by Grimm /2/, who indicated that, for a given pressure of the discharge gas, the discharge current can be limited to an upper value with a large change in the discharge voltage. As a result of this characteristic, the Grimm-style glow discharge is particularly stable.

The generation of particles analyzed results from a non-thermal cathode sputtering process. No melting of the surface and accordingly no selective vocalization occur in contrast to arc or spark erosion /18/. A unique feature of the Grimm-style tube lies in the easily controllable sampling caused by the cathode sputtering. The

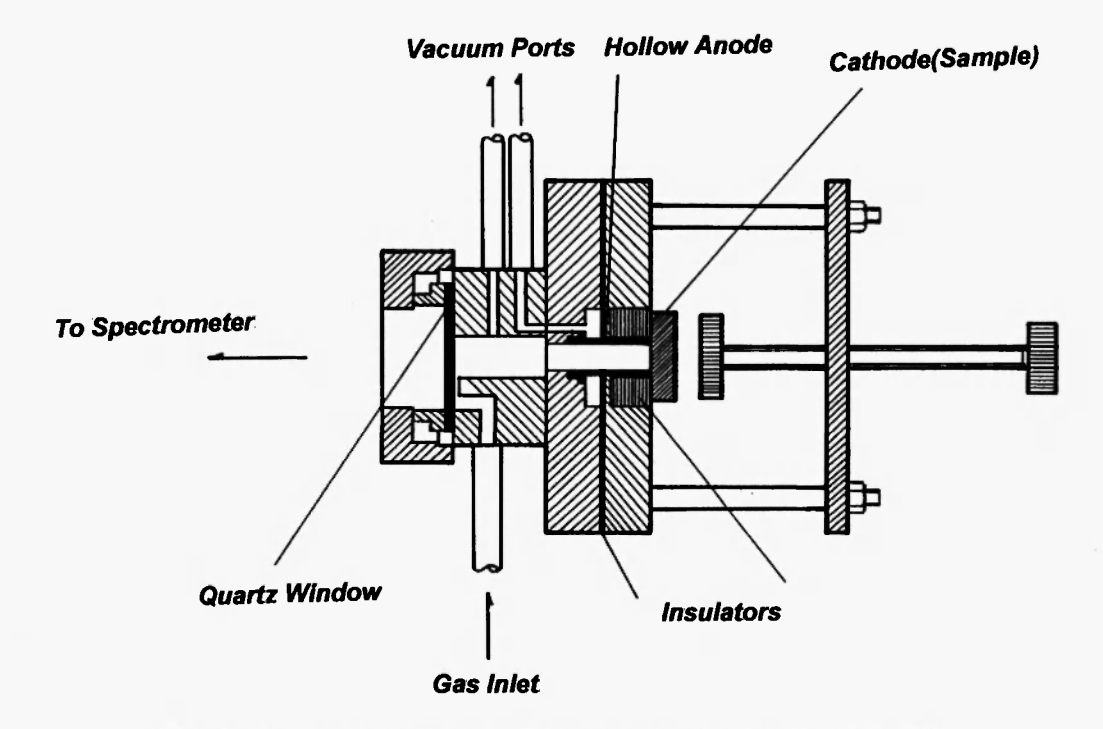


Fig. 6: Cross-section diagram of Grimm-style glow discharge tube /42/.

sampling rate depends on the voltage, the current, and the gas pressure, and is material specific. Information on the in-depth variation of the elemental composition is obtained by analyzing the emission intensities with sputtering time /41,43/.

6. SELECTION OF SPECTRAL LINES

Since the glow discharge plasma is produced in an inert gas at low pressure, it can be used directly as an excitation source in a shorter wavelength region than 200 nm. This allows the detection of non-metals such as oxygen, nitrogen, and hydrogen, whose atomic resonance emission lines lie in the vacuum ultraviolet wavelength region, although a standard air-path spectrometer cannot be employed because of wavelength absorption of less than 190 nm by oxygen in the atmosphere.

Table 4 summarizes sensitive emission lines by elements which are available in the glow discharge spectroscopy, especially with the Grimm-style glow discharge tube. In most of the elements, resonance emission lines of the neutral atom are sufficiently intense to be employed for the qualitative analysis; in

some of the elements, strong emission lines of the singly-ionized atom are observed. These particular ionic lines are selectively excited through charge transfer collisions between analyte atoms and plasma gas ions (Eq. (4)). Such ionic lines can emanate from a particular plasma whereas they are hardly excited with the other gases /23/. This effect is explained by good matching in the excitation energy between the particles involved in the collisions. For example, the Cu II 248.58 nm and Cu II 270.32 nm lines can be excited by the neon plasma, not by the argon or the nitrogen plasma.

Emission lines of fluorine are hardly excited by the argon glow discharge plasma; however, not only the atomic lines but also the ionic lines can be observed with neon. The neon plasma should therefore be employed for fluorine analysis, and the F I 685.60 nm line is recommended as an analytical line /44/.

It was believed that, in the glow discharge plasma, self-absorption was less important than in the other plasmas for analytical spectrometry /3/. However, atomic resonance lines, such as the Cu I 324.74 nm line, might suffer from self-absorption to a certain extent /45, 46/. In this case, the use of ionic emission lines, which are essentially free of self-absorption, is a suitable means for obtaining better linearity of the calibration curves /46/.

Table 4
Sensitive emission lines excited by the Grimm-style glow discharges using several plasma gases

Emission Lines	Assignment		Plasma Gas
	Upper Level (eV)	Lower Level(eV)	
Hydrogen			
H I 121.51	$2p^{2}\mathbf{P}_{1/2,3/2}$ (10.198)	$1s^2S_{1/2}(0.000)$	Ar, Ar+He
H 1 656.28	$3p^2\mathbf{P}_{1/2,3/2}$ (12.087)	$2s^2S_{1/2}(10.199)$	Ar, Ar+He
Lithium			
Li I 610.36	$3d^2\mathbf{D}_{3/2}(3.878)$	$2p^{2}\mathbf{P}_{3/2.1/2}(1.848)$	Ar, Ne, N ₂
Li I 670.79	$2p^{2}\mathbf{P}_{1/2,3/2}(1.848)$	$2s^2S_{1/2}(0.000)$	Ar, Ne, N_2
Carbon			
C I 193.09	$3s^{1}\mathbf{P}_{1}(7.685)$	$2p^{1}\mathbf{D}_{2}(1.264)$	Ar, Ae+He
C I 165.70	$3s^3P_2(7.488)$	$2p^{3}\mathbf{D}_{2}(0.005)$	Ar, Ar+He

Table 4 (continued)			
C I 247.86	$3s^{1}\mathbf{P}_{1}$ (7.685)	$2p^{1}S_{0}(2.684)$	Ar, Ar+He
Nitrogen			
N 1 174.27	$3s^{2}\mathbf{P}_{3/2}(10.690)$	$2p^{2}\mathbf{P}_{1/2}(3.576)$	Ar, Ar+He
N 1 174.52	$3s^2 \mathbf{P}_{1/2} (10.679)$	$2p^{2}\mathbf{P}_{1/2}(3.576)$	Ar, Ar+He
Oxygen			
O 1 130.22	$3s^3S_1(9.521)$	$2p^{3}\mathbf{P}_{2}(0.000)$	Ar, Ar+He
O 1 130.48	$3s^3S_1(9.521)$	$2p^{3}\mathbf{P}_{1}(0.020)$	Ar, Ar+He
O I 777.20	$3p^{5}\mathbf{P}_{3}(10.741)$	$3s ^5S_2 (9.146)$	Ar, Ar+He
O I 777.42	$3p^{5}\mathbf{P}_{2}(10.740)$	$3s ^5S_2 (9.146)$	
Fluorine			
F I 685.60	3p ⁴ D _{7/2} (14.504)	$3s^4\mathbf{P}_{5/2}(12.696)$	Ne
F I 690.25	$3p^4 \mathbf{D}_{5/2} (14.526)$	$3s^4\mathbf{P}_{3/2}(12.731)$	Ne
Sodiu m			
Na I 330.24	$4p^{2}\mathbf{P}_{3/2}(3.753)$	$3s^2S_{1/2}(0.000)$	Ar, Ne, N ₂
Na I 330.30	$4p^{2}\mathbf{P}_{1/2}(3.752)$	$3s^2 S_{1/2}(0.000)$	Ar, Ne, N ₂
Na I 588.99	$3p^{2}\mathbf{P}_{3/2}(2.104)$	$3s^2 S_{1/2}(0.000)$	Ar, Ne, N ₂
Na I 589.59	$3p^2\mathbf{P}_{1/2}(2.102)$	$3s^2S_{1/2}(0.000)$	Ar, Ne, N ₂
Magnesium	_	_	
Mg II 279.55	$3p^{2}\mathbf{P}_{3/2}(4.434)$	$3s^2S_{1/2}(0.000)$	Ar, Ne
Mg II 280.27	$3p^{2}\mathbf{P}_{1/2}$ (4.422)	$3s^{2}S_{1/2}(0.000)$	Ar, Ne
Mg 1 285.21	$3p^{1}\mathbf{P}_{1}(4.346)$	$3s^{1}S_{0}(0.000)$	Ar, Ne
Aluminum			
Al II 167.08	$3p^{1}\mathbf{P}_{1}(7.420)$	$3s^{1}S_{0}(0.000)$	Ne, Ar+He, Ar
Al II 172.13	$3d^{3}\mathbf{D}_{2.1}$ (11.847)	$3p^{3}\mathbf{P}_{1}(4.644)$	Ne, Ar+He
АІ II 172.50	$3d_{3}^{3}\mathbf{D}_{23}$ (11.847)	$3p^{3}\mathbf{P}_{2}$ (4.659)	Ne, Ar+He
Al II 186.23	$4s^{3}S_{1}(11.316)$	$3p^{3}\mathbf{P}_{2}(4.659)$	Ne, Ar+He
Al II 199.05	$3d^{1}\mathbf{D}_{2}$ (13.649)	$3p^{1}\mathbf{P}_{1}(7.420)$	Ne, Ar+He
Al 1 236.80	$4d^{2}\mathbf{D}_{3/2} (4.826)$	$3p^{2}\mathbf{P}_{1/2}(0.000)$	Ar, Ar+He
Al 1257.51	$4d^{2}\mathbf{D}_{5/2}(4.827)$	$3p^2\mathbf{P}_{3/2}(0.014)$	Ar, Ar+He
Al II 263.15	$4f^{1}\mathbf{F}_{3}(15.308)$	$3p^{1}\mathbf{D}_{2}(10.598)$	Ne
Al 1 308.21	$3d^{2}\mathbf{D}_{3/2}(4.021)$	$3p^{2}\mathbf{P}_{1/2}(0.000)$	Ar, Ar+He, Ne

Table 4 (continued)			
Al I 309.28	$3d^2\mathbf{D}_{5/2.3/2}(4.022)$	$3p^{2}\mathbf{P}_{3/2}(0.014)$	Ar, Ar+He, Ne
Al II 358.66	$4f^{3}\mathbf{F}_{4}$ (15.302)	$3d^{3}\mathbf{D}_{3}$ (11.846)	Ne
Al II 358.72	$4f^3\mathbf{F}_3(15.302)$	$3d^{3}\mathbf{D}_{2}(11.846)$	Ne
Al II 358.75	$4f^{3}\mathbf{F}_{2}$ (15.301)	$3d^{3}\mathbf{D}_{1}(11.847)$	Ne
Al I 394.40	$4s^2S_{1/2}(3.143)$	$3p^{2}\mathbf{P}_{1/2}(0.000)$	Ar, Ar+He, Ne
Al I 396.15	$4s^2S_{1/2}(3.143)$	$3p^2\mathbf{P}_{3/2}(0.014)$	Ar, Ar+He, Ne
Phosphorous			
P 1 177.49	$4s^{4}\mathbf{P}_{5/2}(6.985)$	$3p^4S_{3/2}(0.000)$	Ar, Ar+He
P I 178.28	$4s^{4}\mathbf{P}_{3/2}(6.954)$	$3p^4S_{3/2}(0.000)$	Ar, Ar+He
P I 178.77	$4s {}^{4}\mathbf{P}_{1/2} (6.935)$	$3p^4S_{3/2}(0.000)$	Ar, Ar+He
Sulfur			
S I 180.73	$4s^3S_1(6.860)$	$3p^{3}\mathbf{P}_{2}(0.000)$	Ar, Ar+He
S I 182.03	$4s^3S_1(6.860)$	$3p^{3}\mathbf{P}_{1}(0.049)$	Ar, Ar+He
S I 182.62	$4s^3S_1(6.860)$	$3p^{3}\mathbf{P}_{0}(0.071)$	Ar, Ar+He
S I 190.03	$4s ^5S_2 (6.524)$	$3p^{3}\mathbf{P}_{2}(0.000)$	Ar, Ar+He
Chlorine			
Cl I 137.95	$4s^4 \mathbf{P}_{3/2} (8.987)$	$3p^2\mathbf{P}_{3/2}(0.000)$	Ar, Ar+He
Cl I 138.97	$4s^{4}\mathbf{P}_{5/2}(8.921)$	$3p^{2}\mathbf{P}_{3/2}(0.000)$	Ar, Ar+He
Cl I 138.99	$4s^{4}\mathbf{P}_{1/2}(9.029)$	$3p^2\mathbf{P}_{1/2}(0.109)$	Ar, Ar+He
Potassium			
K I 404.41	$5p^{2}\mathbf{P}_{3/2}(3.065)$	$4s^2S_{1/2}(0.000)$	Ar, Ne, N ₂
K 1 404.72	$5p^2\mathbf{P}_{1/2}(3.062)$	$4s^{2}S_{1/2}(0.000)$	Ar, Ne, N ₂
Calcium			
Ca II 393.37	$4p^{2}\mathbf{P}_{3/2}(3.151)$	$4s^2S_{1/2}(0.000)$	Ar, Ne, N ₂
Ca II 396.85	$4p^{2}\mathbf{P}_{1/2}(3.123)$	$4s^2S_{1/2}(0.000)$	Ar, Ne, N ₂
Ca I 422.67	$4p^{1}\mathbf{P}_{1}(2.932)$	$4s^{1}S_{0}(0.000)$	Ar, Ne, N ₂
Titanium			
Ті ІІ 282.81	$4d^{4}\mathbf{H}_{13/2}(8.132)$	$4p^4G_{11/2}(3.749)$	Ar, Ne
Ti II 295.46	$4d^{2}\mathbf{H}_{11/2}(8.503)$	$4p^{2}G_{9/2}(4.308)$	Ar, Ne
Ti II 295.88	$4d^{2}\mathbf{H}_{9/2}(8.472)$	$4p^{2}G_{7/2}(4.283)$	Ar, Ne
Ті П 308.80	$4p^{4}\mathbf{D}_{7/2}(4.063)$	$4s^{4}\mathbf{F}_{9/2}(0.049)$	Ar, Ar+He, Ne

Table 4 (continued)			
Ti II 308.99	$5s^4\mathbf{F}_{9/2}(7.761)$	$4p^4G_{11/2}(3.749)$	Ar, Ne
Ti II 323.45	$4p^{4}\mathbf{F}_{9/2}(3.881)$	$4s^4\mathbf{F}_{9/2}(0.049)$	Ar, Ar+He, Ne
Ti II 323.66	$4p^{4}\mathbf{F}_{7/2}(3.858)$	$4p^{4}\mathbf{F}_{7/2}(0.028)$	Ar, Ar+He, Ne
Ti II 334.19	$4p^{2}G_{7/2}(4.283)$	$4s^2\mathbf{F}_{5/2}(0.574)$	Ar, Ar+He, Ne
Ті II 334.94	$4p^{4}G_{11/2}(3.749)$	$4s^4\mathbf{F}_{9/2}(0.049)$	Ar, Ar+He, Ne
Ті ІІ 337.28	$4p\ ^4G_{7/2}(3.687)$	$4s^{4}\mathbf{F}_{5/2}(0.012)$	Ar, Ar+He, Ne
Ti II 338.38	$4p\ ^4\mathbf{G}_{5/2}(3.663)$	$4s^{4}\mathbf{F}_{3/2}(0.000)$	Ar, Ar+He, Ne
Ti 1 365.35	$4p^{3}G_{5}(3.441)$	$4s^{3}\mathbf{F}_{4}(0.048)$	Ar, Ar+He
Ti II 368.52	$4p^{2}\mathbf{D}_{3/2}(3.937)$	$4s^{2}\mathbf{F}_{5/2}(0.574)$	Ar, Ar+He, Ne
Ti II 375.93	$4p^{2}\mathbf{F}_{7/2}(3.904)$	$4s^{2}\mathbf{F}_{7/2}(0.607)$	Ar, Ar+He, Ne
Ti II 376.13	$4p^{2}\mathbf{F}_{5/2}(3.869)$	$4s^{2}\mathbf{F}_{5/2}(0.574)$	Ar, Ar+He, Ne
Ti I 398.98	$4p^{3}\mathbf{F}_{3}(3.128)$	$4s^3\mathbf{F}_3(0.021)$	Ar, Ar+He
Ti 1 399.86	$4p^{3}\mathbf{F}_{4}(3.148)$	$4s^3\mathbf{F}_4(0.048)$	Ar, Ar+He
Chromium			
Cr II 267.72	$4p^{6}\mathbf{D}_{7/2}(6.155)$	4s $^{6}\mathbf{D}_{7/2}(1.526)$	Ar, Ne
Cr II 283.56	$4p^{6}\mathbf{F}_{11/2}(5.920)$	4s $^{6}\mathbf{D}_{9/2}(1.549)$	Ar, Ne
Cr II 284.32	$4p^{6}\mathbf{F}_{9/2}(5.885)$	$4s^{6}\mathbf{D}_{7/2}(1.526)$	Ar, Ne
Cr 1 357.87	$4p^{7}\mathbf{P}_{4}(3.463)$	4s 7 S ₃ (0.000)	Ar, Ne
Cr I 359.35	$4p^{7}\mathbf{P}_{3}(3.449)$	$4s^{7}S_{3}(0.000)$	Ar, Ne
Cr 1 360.53	$4p^{7}\mathbf{P}_{2}(3.438)$	$4s^{7}S_{3}(0.000)$	Ar, Ne
Cr 1 425.43	$4p^{7}\mathbf{P}_{4}(2.913)$	$4s^{7}S_{3}(0.000)$	Ar, Ne, Ar+He
Cr I 427.48	$4p^{7}P_{3}(2.899)$	$4s^{7}S_{3}(0.000)$	Ar, Ne, Ar+He
Cr I 428.97	$4p^{7}P_{2}(2.889)$	$4s^{7}S_{3}(0.000)$	Ar, Ne, Ar+He
Iron			
Fe II 160.85	4p ⁶ P _{7/2} (7.708)	$4s^6 \mathbf{D}_{9/2}(0.000)$	Ar, Ar+He
Fe II 161.85	$4p^{6}\mathbf{P}_{7/2}(7.708)$	$4s^{6}\mathbf{D}_{7/2}(0.048)$	Ar, Ar+He
Fe II 162.17	$4p^{6}\mathbf{P}_{50}(7.693)$	$4s^{6}\mathbf{D}_{30}(0.048)$	Ar, Ar+He
Fe II 162.92	$4p^{6}\mathbf{P}_{5/2}(7.693)$	$4s^{6}\mathbf{D}_{5/2}(0.083)$	Ar, Ar+He
Fe II 183.36	$4p^{8}P_{7/2}(13.246)$	$4s^{8}P_{5/2}(6.484)$	Ne
Fe II 184.32	$4p^{8}P_{7/2}(13.246)$	$4s^{8}\mathbf{P}_{7/2}(6.519)$	Ne
Fe II 185.63	$4p^{8}P_{7/2}(13.246)$	$4s {}^{8}\mathbf{P}_{9/2}(6.519)$	Ne
Fe II 234.43	$4p^{6}\mathbf{D}_{3/2}(5.408)$	$4s^{6}\mathbf{D}_{1/2}(0.121)$	Ne, Ar+He, Ar
Fe II 238.20	$4p^{6}\mathbf{F}_{11/2}(5.203)$	4s $^{6}\mathbf{D}_{9/2}(0.000)$	Ne, Ar+He, Ar
Fe II 239.56	$4p^{6}\mathbf{F}_{9/2}(5.221)$	$4s^{6}\mathbf{D}_{7}(0.048)$	Ne, Ar+He, Ar
Fe II 252.96	$4p^{4}\mathbf{P}_{3/2}(7.604)$	$4s^{4}\mathbf{P}_{3/2}(2.704)$	Ar, Ar+He, Ne

Table 4 (continued)			
Fe II 257.30	$4p^{6}\mathbf{P}_{7/2}(7.708)$	$4s^6S_{5/2}(2.891)$	Ar, Ar+He, Ne
Fe II 259.94	$4p^{6}\mathbf{D}_{9/2}(4.768)$	$4s^{6}\mathbf{D}_{9/2}(0.000)$	Ne, Ar+He, Ar
Fe II 273.95	$4p^{2}I_{11/2}(7.769)$	$4s^2\mathbf{H}_{11/2}(3.245)$	Ar, Ar+He, Ne
Fe II 275.33	$4p^{2}I_{11/2}(7.769)$	$4s^2\mathbf{H}_{9/2}(3.267)$	Ar, Ar+He, Ne
Fe II 275.57	$4p^{4}\mathbf{F}_{9/2}(5.484)$	$4s^4 \mathbf{D}_{7/2}(0.986)$	Ne, Ar+He, Ar
Fe II 276.75	$4p^{2}I_{13/2}(7.723)$	$4s^2 \mathbf{H}_{11/2}(3.245)$	Ar, Ar+He, Ne
Fe I 344.06	$4p^{5}\mathbf{P}_{3}(3.602)$	$4s^{5}\mathbf{D}_{4}(0.000)$	Ar
Fe 1 344.10	$4p^{5}\mathbf{P}_{2}(3.654)$	$4s^{5}\mathbf{D}_{3}(0.052)$	Ar
Fe I 371.99	$4p^{5}\mathbf{F}_{1}(3.332)$	$4s^5 \mathbf{D}_4 (0.000)$	Ar, Ne
Fe 1 373.71	$4p^{5}\mathbf{F}_{4}(3.368)$	$4s^{5}\mathbf{D}_{3}(0.052)$	Ar, Ne
Fe 1 374.56	$4p^{5}\mathbf{F}_{3}$ (3.396)	$4s ^5\mathbf{D}_2 (0.087)$	Ar, Ne
Fe 1 374.83	$4p^{5}\mathbf{F}_{2}(3.417)$	$4s^{5}\mathbf{D}_{1}(0.110)$	Ar, Ne
Cobalt			
Co II 229.20	4p ⁵ D ₄ (7.611)	$4s^{5}\mathbf{P}_{3}(2.203)$	Ar, Ar+He, Ne
Co II 233.79	$4p {}^{3}G_{3}(8.081)$	4s ${}^{3}\mathbf{G}_{3}(2.779)$	Ar, Ar+He, Ne
Co II 238.18	$4p^{3}\mathbf{H}_{6}(7.995)$	$4s {}^{3}G5(2.681)$	Ar, Ar+He, Ne
Co II 239.74	$4p^{3}\mathbf{D}_{3}(6.387)$	$4s^{3}\mathbf{F}_{4}(1.217)$	Ar, Ar+He, Ne
Со II 241.60	$4p^{3}\mathbf{H}_{4}(7.909)$	$4s^{3}\mathbf{G}_{3}(2.779)$	Ar, Ar+He, Ne
Co II 242.07	$4p^{3}\mathbf{H}_{5}(7.849)$	$4s {}^{3}\mathbf{G}_{4}(2.729)$	Ar, Ar+He, Ne
Co II 251.12	$4p^{1}\mathbf{H}_{5}(8.053)$	$4s {}^{1}G4(3.118)$	Ar, Ar+He, Ne
Co II 253.01	$4p^{3}\mathbf{D}_{3}(7.884)$	$4s^{3}\mathbf{P}_{2}(2.985)$	Ar, Ar+He, Ne
Co II 254.67	$4p^{1}G_{4}(7.985)$	$4s {}^{1}G_{4}(3.118)$	Ar, Ar+He, Ne
Co II 258.03	$4p^{3}G_{5}(6.020)$	$4s^{3}\mathbf{F}_{4}(1.217)$	Ar, Ar+He, Ne
Co 1 340.51	$4p^{4}\mathbf{F}_{9/2}(4.072)$	$4s^{4}\mathbf{F}_{9/2}(0.432)$	Ar, Ne
Co I 341.23	$4p^{2}\mathbf{G}_{9/2}(4.146)$	$4s^{4}\mathbf{F}_{7/2}(0.514)$	Ar, Ne
Co 1 341.26	$4p^{4}\mathbf{D}_{7/2}(3.632)$	$4s^{4}\mathbf{F}_{9/2}(0.000)$	Ar, Ne
Co 1 345.35	$4p {}^{4}\mathbf{G}_{11/2}(4.021)$	$4s^{4}\mathbf{F}_{9/2}(0.432)$	Ar, Ne
Co I 346.58	$4p^{4}\mathbf{G}_{11/2}(3.576)$	$4s^{4}\mathbf{F}_{9/2}(0.000)$	Ar, Ne
Co 1 350.23	$4p^{4}\mathbf{D}_{7/2}(3.971)$	$4s^{4}\mathbf{F}_{9/2}(0.432)$	Ar, Ne
AT: 1 1			
Nickel	4 25 (7.050)	2.1270 (0.000)	A A . TT . D.T
Ni II 170.96	$4p^{2}\mathbf{F}_{5/2}(7.252)$	$3d^{2}\mathbf{D}_{5/2}(0.000)$	Ar, Ar+He, Ne
Ni II 172.11	$4p^{4}\mathbf{F}_{9/2}(13.532)$	$4s^{4}\mathbf{F}_{9/2}(6.329)$	Ne
Ni II 172.96	4p (13.641)	$4s^{4}\mathbf{F}_{7/2}(6.473)$	Ne
Ni II 173.49	$4p^{4}\mathbf{F}_{7/2}(13.619)$	$4s^{4}\mathbf{F}_{7/2}(6.473)$	Ne
Ni II 174.16	$4p^{2}\mathbf{D}_{5/2}(7.119)$	$3d^2\mathbf{D}_{5/2}(0.000)$	Ar, Ar+He, Ne

Table 4	(continued)
---------	-------------

Ni II 174.83	$4p^{2}\mathbf{D}_{3/2}(7.278)$	$3d^2\mathbf{D}_{3/2}(0.187)$	Ar, Ar+He, Ne
Ni II 178.86	$4p^{2}\mathbf{D}_{5/2}(7.119)$	$3d^2\mathbf{D}_{3/2}(0.187)$	Ar, Ar+He, Ne
Ni II 212.86	$4p^{2}\mathbf{F}_{7/2}(7.077)$	$4s^{4}\mathbf{F}_{5/2}(1.254)$	Ne, Ar+He, Ar
Ni 11 216.56	$4p^{4}\mathbf{F}_{9/2}(6.764)$	$4s^{4}\mathbf{F}_{9/2}(1.041)$	Ne, Ar+He, Ar
Ni II 217.51	$4p^{4}\mathbf{F}_{5/2}(6.952)$	$4s^{4}\mathbf{F}_{5/2}(1.254)$	Ne, Ar+He, Ar
Ni II 220.14	$4p^{4}\mathbf{F}_{5/2}(6.952)$	$4s^4\mathbf{F}_{3/2}(1.322)$	Ne, Ar+He, Ar
Ni II 221.65	$4p ^4\mathbf{G}_{11/2}(6.633)$	$4s^{4}\mathbf{F}_{9/2}(1.041)$	Ne, Ar+He, Ar
Ni II 225.38	$4p^{4}\mathbf{G}_{5/2}(6.821)$	$4s^4\mathbf{F}_{3/2}(1.322)$	Ne, Ar+He, Ar
Ni II 227.88	$4p^{2}\mathbf{D}_{5/2}(7.119)$	$4s^2\mathbf{F}_{7/2}(1.680)$	Ar, Ar+He, Ne
Ni II 228.71	$4p^{2}\mathbf{D}_{3/2}(7.278)$	$4s^{2}\mathbf{F}_{5/2}(1.859)$	Ar, Ar+He, Ne
Ni II 229.83	$4p^{2}\mathbf{F}_{5/2}(7.252)$	$4s^{2}\mathbf{F}_{5/2}(1.859)$	Ar, Ar+He, Ne
Ni 1 232.00	$4p^{3}G_{5}(5.342)$	$4s^3\mathbf{F}_4(0.000)$	Ar, Ar+He, Ne
Ni II 237.60	$4p^{4}\mathbf{D}_{5/2}(6.539)$	$4s^{4}\mathbf{F}_{3/2}(1.322)$	Ne, Ar+He, Ar
Ni II 239.45	$4p^{2}\mathbf{G}_{9/2}(6.856)$	$4s^2\mathbf{F}_{7/2}(1.680)$	Ne, Ar+He, Ar
Ni II 241.61	$4p^{2}\mathbf{G}_{7/2}(6.989)$	$4s^{2}\mathbf{F}_{5/2}(1.859)$	Ar, Ar+He, Ne
Ni II 251.09	4p ⁴ G _{9/2} (6.616)	$4s^2\mathbf{F}_{7/2}(1.680)$	Ne, Ar+He, Ar
Ni I 341.48	$4p^{3}\mathbf{F}_{4}(3.655)$	$4s^3\mathbf{D}_3(0.025)$	Ar, Ne
Ni 1 343.36	$4p^{3}\mathbf{F}_{3}(3.635)$	$4s^3\mathbf{D}_3(0.025)$	Ar, Ne
Ni 1 344.63	4p (3.706)	$4s^3\mathbf{D}_2(0.109)$	Ar, Ne
Ni 1 345.85	$4p^{3}\mathbf{F}_{2}(3.796)$	$4s^3\mathbf{D}_1(0.212)$	Ar, Ne
Ni 1 349.30	$4p^{3}\mathbf{P}_{1}(3.657)$	$4s^3\mathbf{D}_2(0.109)$	Ar, Ne
Ni I 351.50	$4p^{3}\mathbf{F}_{3}(3.635)$	$4s^3\mathbf{D}_2(0.109)$	Ar, Ne
Ni 1 352.45	$4p^{3}\mathbf{P}_{2}(3.542)$	$4s^3\mathbf{D}_3(0.025)$	Ar, Ne
Copper			
Cu II 199.96	$4p^{i}\mathbf{F}_{3}(8.917)$	$4s^3\mathbf{D}_3(2.719)$	Ar+He, Ne
Cu II 203.59	$4p^{3}\mathbf{D}_{1}(9.063)$	$4s^3 \mathbf{D}_1 (2.975)$	Ar+He, Ne
Cu II 204.38	$4p^{3}\mathbf{D}_{3}(8.783)$	$4s^3\mathbf{D}_3(2.719)$	Ar+He, Ne
Cu II 212.30	$4p^{1}\mathbf{P}_{1}(9.125)$	$4s^{1}\mathbf{D}_{2}(3.256)$	Ar+He, Ne
Cu II 212.60	$4p^{1}\mathbf{D}_{2}(9.094)$	$4s^{1}\mathbf{D}_{2}(3.256)$	Ar+He, Ne
Cu II 217.94	$4p^{3}\mathbf{F}_{2}(8.662)$	$4s^3 \mathbf{D}_1 (2.975)$	Ar+He, Ne
Cu II 221.81	$4p^{3}\mathbf{P}_{1}(8.420)$	$4s^3\mathbf{D}_2(2.833)$	Ar+He, Ne, Ar
Cu II 222.89	$4p^{3}P_{0}(8.536)$	$4s^3 \mathbf{D}_1 (2.975)$	Ar+He, Ne, Ar
Cu II 224.26	$4p^{3}\mathbf{D}_{3}(8.783)$	$4s^{-1}\mathbf{D}_{2}(3.256)$	Ar+He, Ne
Cu II 224.70	$4p^{3}P_{2}(8.235)$	$4s^3\mathbf{D}_3(2.719)$	Ar, Ne
Cu II 248.58	$5s^3\mathbf{D}_1(13.649)$	$4p^{3}\mathbf{F}_{2}(8.662)$	Ne
Cu II 270.10	$5s^{-1}\mathbf{D}_{2}(13.683)$	$4p^{1}\mathbf{D}_{2}(9.094)$	Ne
	_	-	

Table 4 (con	tinued)			
Cu II 270.3	$5s^3\mathbf{D}$	1 (13.649)	$4p^{3}\mathbf{D}_{1}(9.063)$	Ne
Cu II 271.3	$5s^{3}\mathbf{D}$	2 (13.432)	$4p^{3}\mathbf{D}_{2}(8.864)$	Ne
Cu II 271.8	38 5s 1 D	2 (13.683)	$4p^{1}\mathbf{P}_{1}(9.124)$	Ne
Cu I 324.73	$4p^2\mathbf{P}$	_{3/2} (3.817)	$4s^2S_{1/2}(0.000)$	Ar, Ne, N,
Cu I 327.39	9 4p2P	(3.786)	$4s^2S_{1/2}(0.000)$	Ar, Ne, N_2
Cu I 515.32	$2 4d^2\mathbf{D}$	_{3/2} (6.191)	$4p^{2}\mathbf{P}_{1/2}(3.786)$	Ar, N ₂
Cu I 521.82	$2 4d^2\mathbf{D}$	o _{5/2} (6.192)	$4p^2\mathbf{P}_{3/2}(3.817)$	Ar, N_2
Zinc				
Zn II 202.5	_ `		$4s^2S_{1/2}(0.000)$	Ar, Ne, Ar+He
Zn II 206.2	·		$4s^2 S_{1/2}(0.000)$	Ar, Ne, Ar+He
Zn II 206.4	_		$4p^{2}\mathbf{P}_{1/2}(6.011)$	He+Ar, Ne
Zn II 210.2			$4p^{2}\mathbf{P}_{3/2}(6.119)$	He+Ar, Ne
Zn 1 213.86			$4s^{1}S_{0}(0.000)$	Ar, Ne, N ₂
Zn 1 307.59	=		$4s^{1}S_{0}(0.000)$	Ar, Ne, N ₂
Zn 1 328.23		-	$4p^{3}\mathbf{P}_{0}(4.006)$	Ar, Ar+He
Zn I 330.26			$4p^{3}\mathbf{P}_{1}(4.030)$	Ar, Ar+He
Zn 1 330,29			$4p^{3}\mathbf{P}_{1}(4.030)$	Ar, Ar+He
Zn 1 334.50		•	$4p^{3}\mathbf{P}_{2}(4.078)$	Ar, Ar+He
Zn 1 334.56			$4p^{3}\mathbf{P}_{2}(4.078)$	Ar, Ar+He
Zn 1 472,22				Ar, N ₂ , Ar+He
Zn 1 481.06	$5 5s^3 \mathbf{S}_1$	(6.654)	$4p^{3}\mathbf{P}_{2}(4.078)$	Ar, N ₂ , Ar+He
Silver	- 1-			
Ag II 228.0				He+Ar, Ar, Ne
Ag II 241.3				He+Ar, Ar, Ne
Ag II 243.7			$5s^{3}\mathbf{D}_{3}$ (4.856)	He+Ar, Ar, Ne
Ag II 271.1			. 4 .	He+Ar
Ag II 293.4			• , 3 ` /	He+Ar
Ag I 328.07				Ar, Ne, N ₂
Ag I 338.29		(3.664)		Ar, Ne, N ₂
Ag I 520.91		(6.043)		Ar, Ne, N ₂
Ag I 546.55	$5 5d^2\mathbf{D}$	(6.046)	$5p^2\mathbf{P}_{3/2}(3.778)$	Ar, Ne, N ₂
m·				
Tin	2 - 2-	(7.270)	c 2n (0.505)	4 37
Sn II 181.1			$5p^{2}\mathbf{P}_{3/2}(0.527)$	Ar, Ne
Sn II 183.1	8 5p D	_{3/2} (7.296)	$5p^{2}\mathbf{P}_{3/2}(0.527)$	Ar, Ne

Table 4 (continued)

Sn II 189.99	$6s^2S_{1/2}(7.053)$	$5p^{2}\mathbf{P}_{3/2}(0.527)$	Ar, Ne
Sn 1 303.41	$6s^{3}\mathbf{P}_{0}(4.295)$	$5p^{3}\mathbf{P}_{1}(0.210)$	Ar, Ne, N ₂
Sn 1 317.50	$6s^{3}\mathbf{P}_{1}(4.329)$	$5p^{3}\mathbf{P}_{2}(0.425)$	Ar, Ne, N ₂
Sn 1 326.23	$6s^{1}\mathbf{P}_{1}(4.867)$	$5p^{1}\mathbf{D}_{2}(1.068)$	Ar, Ne, N ₂
Sn II 328.33	4f ${}^{2}\mathbf{F}_{5/2}$ (11.071)	$5p^{2}\mathbf{D}_{3/2}(7.296)$	Ne
Sn II 335.15	4f ${}^{2}\mathbf{F}_{5/2}$ (11.071)	$5p^{2}\mathbf{D}_{5/2}(7.372)$	Ne
Sn II 335.22	$4f^{2}\mathbf{F}_{7/2}(11.070)$	$5p^{2}\mathbf{D}_{5/2}(7.372)$	Ne
Lead			
Pb II 172.68	$6p^{4}\mathbf{P}_{1/2}(7.180)$	$6p^{2}\mathbf{P}_{1/2}(0.000)$	Ar, Ne
Pb II 179.67	$6d^2\mathbf{D}_{3/2}(8.646)$	$6p^{2}\mathbf{P}_{1/2}(0.000)$	Ar, Ne
Pb II 182.21	$6d^{2}\mathbf{D}_{5/2}(8.550)$	$6p^{2}\mathbf{P}_{3/2}(1.746)$	Ar, Ne
Pb 1 280.20	$6d^{3}\mathbf{F}_{3}(5.744)$	$6p^{3}\mathbf{P}_{2}(1.320)$	Ar, Ne, N ₂
Pb 1 405.78	$7s^{3}\mathbf{P}_{1}(4.375)$	$6p^{3}\mathbf{P}_{2}(1.320)$	Ar, Ne, N_2
Pb II 424.51	$5f^{2}\mathbf{F}_{7/2}(11.470)$	$6d^2\mathbf{D}_{5/2}(8.550)$	Ne
РЬ II 438.69	$5f^{2}\mathbf{F}_{5/2}(11.472)$	$6p^2\mathbf{D}_{3/2}(8.646)$	Ne

REFERENCES

- 1. W. Grimm, Naturwissenschaften, 54, 586 (1967).
- 2. W. Grimm, Spectrochim. Acta, 23B, 443 (1968).
- 3. R. Mavrodineau, J. Res. Natl. Bur. Stand, 89, 143 (1984).
- J.A.C. Broekaert, J. Anal. Atom. Spectrom., 2, 537 (1987).
- 5. S. Carol, J. Anal. Atom. Spectrom., 2, 661 (1987).
- 6. J. Plucker, Ann. Physik, 103, 88 (1958).
- 7. R. Behrisch (Ed.), Sputtering by Particle Bombardment I, Springer-Verlag, Berlin, 1981.
- 8. B. Chapman, *Glow Discharge Processes*, John Wiley & Sons, New York, 1980.
- J.S. Chang, R.M. Hobson, Y. Ichikawa and T. Kaneda, Atomic and Molecular Processes in Ionized Gases, Tokyo Denki Univ. Press, Tokyo, 1982
- G. Francis, Handbuck der Physik, Vol. 22, Springer-Verlag, Berlin, 1956.
- 11. F.M. Penning, *Philips Technical Library*, Eindhoven, 1957.

- A. von Engel, *Ionized Gases*, Clarendon Press, Oxford, 1965.
- 13. M. Dogan, K. Laqua and H. Massman, Spectrochim. Acta, 26B, 631 (1971).
- 14. M. Dogan, K. Laqua and H. Massman, Spectrochim. Acta, 27B, 65 (1972).
- 15. N.P. Ferreira, J.A. Strauss and H.G.C. Human, Spectrochim. Acta, 38B, 899 (1983).
- 16. K. Hatta, Gas Discharges (Kitai Hohden), Kindai-Kagakusya, Tokyo, 1968.
- N.I. Uzelac and F. Leis, Spectrochim. Acta, 47B, 877 (1992).
- 18. P.W.J.M. Boumans, *Theory of Spectrochemical Excitations*, Plenum Press, New York, 1966.
- G. Herzberg, Atomic Spectra and Atomic Structure, Dover Publications, New York, 1944.
- 20. A. Corney, *Atomic and Laser Structure*, Oxford Science Publications, Oxford, 1977.
- C.E. Moore, Atomic Energy Levels, Vol. 1, NBS circular 467, 1949.
- 22. O.S. Duffendach and J.G. Black, *Phys. Rev.*, 34, 35 (1929).

- 23. K. Wagatsuma, Bunseki Kagaku, 41, 353 (1992).
- 24. K. Wagatsuma and K. Hirokawa, *Anal. Chem.*, **57**, 2901 (1985).
- 25. K. Wagatsuma and K. Hirokawa, *Spectrochim. Acta*, 46B, 269 (1991).
- 26. K. Wagatsuma and K. Hirokawa, Spectrochim. Acta, 51B, 349 (1996).
- 27. E.B.M. Steers and R.J. Fielding, *J. Anal. Atom. Spectrom.*, 2, 239 (1987).
- F.J. de Hoog, J.R. McNeil and G.J. Collins, J. Appl. Phys., 48, 3701 (1977).
- 29. H.J. Eichler, H.J. Koch, J. Salk and G. Schafer, *IEEE.J. Quant. Electron.*, QE15, 908 (1979).
- 30. K. Wagatsuma and K. Hirokawa, *Spectrochim.* Acta, 48B, 1039 (1993).
- 31. J.L. Vossen and J.A. Cuomo, *Thin Film Processes*, Academic Press, London, 1978.
- 32. G. Betz and G.K. Wehner, in: Sputtering by Particle Bombardment II, R. Behrisch (Ed.), Springer-Verlag, Berlin, 1981.
- 33. P. Sigmund, in: Sputtering by Particle Bombardment II, R. Behrisch (Ed.), Springer-Verlag, Berlin, 1981.
- N. Laegreid and G.K. Wehner, J. Appl. Phys., 32, 365 (1961).

- D. Rosenberg and G.K. Wehner, J. Appl. Phys.,
 33, 1842 (1962).
- K. Wagatsuma and K. Hirokawa, Anal. Chem., 56, 412 (1984).
- K. Wagatsuma and K. Hirokawa, Anal. Chem., 56, 2024 (1984).
- Y. Ohashi, Y. Yamamoto, K. Tsunoyama and H. Kishidaka, SIA Surf. Interface Anal., 3, 134 (1981).
- C.J. Belle and J.D. Johnson, *Appl. Spectrosc.*, 27, 118 (1973).
- K.H. Koch, M. Kretschmer and D. Grunenberg, *Mikrochim. Acta*, 2, 225 (1983).
- 41. W.B. Teo and K. Hirokawa, SIA Surf. Interface Anal., 11, 421 (1988).
- 42. K. Wagatsuma and K. Hirokawa, SIA Surf. Interface Anal., 6, 167 (1984).
- 43. A. Bengtson, Spectrochim. Acta, 40B, 631 (1985).
- K. Wagatsuma, K. Hirokawa and N. Yamashita, Anal. Chim. Acta, 324, 147 (1996).
- C.D. West and H.G.C. Human, Spectrochim. Acta, 31B, 81 (1976).
- K. Wagatsuma, T. Kuwabara and K. Hirokawa, *Anal. Chim. Acta*, 343, 267 (1997).